Hindawi Publishing Corporation
Advances in Mechanical Engineering
Article ID 292973

Research Article

A Numerical Analysis on Nanofluid Mixed Convection in Triangular Cross-Sectioned Ducts Heated by a Uniform Heat Flux

Oronzio Manca,[1] Sergio Nardini,[1] Daniele Ricci,[2] and Salvatore Tamburrino[3]

[1] *Dipartimento di Ingegneria Industriale e dell'Informazione, Seconda Università degli Studi di Napoli, Via Roma 29, 81031 Aversa, Italy*
[2] *Italian Aerospace Research Centre (C.I.R.A.), Via Maiorise snc, 81043 Capua, Italy*
[3] *ENEA C.R. Bologna, Via Martiri di Monte Sole 4, 40129 Bologna, Italy*

Correspondence should be addressed to Oronzio Manca; oronzio.manca@unina2.it

Received 25 August 2014; Accepted 3 November 2014

Academic Editor: Yogesh Jaluria

Copyright © Oronzio Manca et al. This is an open access article distributed under the Creative Commons Attribution License, which permits unrestricted use, distribution, and reproduction in any medium, provided the original work is properly cited.

In this paper, results obtained by the numerical investigation on laminar mixed convection in triangular ducts, filled with nanofluids, are presented in order to evaluate the fluid dynamic and thermal features of the considered geometry by considering Al_2O_3/water based nanofluids. The system is heated by a constant and uniform heat flux also along the perimeter of the triangular duct section in H2 mode as thermal boundary condition and the single-phase model has been assigned for a Reynolds number value equal to 100. Results are given for different nanoparticle volume concentrations and Richardson number values ranging from 0% to 5% and from 0 to 5, respectively. Results, presented for the fully developed regime flow, show the enhancement of average convective heat transfer coefficients values for increasing values of Richardson number and particle fractions. However, wall shear stress and required pumping power profiles increase as expected. The PEC analysis showed that the use of nanofluids in mixed convection seems slightly convenient. It should be underlined that, at the moment, experimental data are not available to compare the numerical proposed model for mixed convection in horizontal triangular ducts with nanofluids.

1. Introduction

Every heat exchanger is virtually a potential candidate to be "enhanced" by means of the available heat transfer enhancement technologies. The goal could consist of size reductions, thermodynamic process efficiency improvement, or cost savings of the designed thermal equipment. Thus, great attention to these issues is paid by the research and industrial fields. The use of the heat transfer enhancement techniques is widely diffused in many applications such as heat exchangers for refrigeration, automotive, aeronautic, and electronic applications, process industry, and solar receiver [1]. Heat exchangers can adopt several solutions and arrangements, featured by differently shaped ducts. Aside from circular ducts, channels having square, rhombic, rectangular, triangular, sinusoidal, and elliptical cross-sections, even with truncated corners or special surfaces, could be employed [2–9]. In particular, the study about triangular sectioned ducts has been widely performed because of their employment in the field of compact heat exchangers [10]. In fact, triangular ducts ensure compactness cost effectiveness by means of low fabrication costs, relatively easy construction, and mechanical strength [11, 12]. Forced convection was predominantly investigated both in laminar flow [13–15] and in turbulent one [16–19]. Furthermore, literature covers different fluids, like gas, liquid, non-Newtonian fluids, and, recently, nanofluids [14, 20, 21]. An experimental approach [4, 17] or analytical [22] and numerical methods [21, 23, 24] have been adopted.

Shah and London [25] performed a huge and exhaustive review about theoretical and experimental analyses on laminar forced convection and heat transfer in noncircular ducts. In particular, their book reported the dynamic and

Downloaded from ade.sagepub.com at University of Otago Library on July 24, 2015

thermal features of different triangular ducts, like equilateral, isosceles, and right triangular ones both in fully developed and in developing flow conditions. For the fully developed flow conditions, they provided Nusselt number values equal to 2.47, 3.111, and 1.892 according to T, H_1, and H_2 boundary conditions, respectively. Aggarwala and Gangal [26] analyzed the behaviour of developing laminar flow in equilateral and right isosceles triangular ducts. Yilmaz and Cihan [27] studied the laminar developed flow in ducts having triangular passages, heated at constant temperature, and presented general equations for heat transfer calculations also for circular, rectangular, elliptical, and parallel plate configurations. The influence of axial conduction on heat transfer was described in [28] and the study was accomplished by means of the Galerkin-based integral method.

Literature is less extended on the mixed or natural convection side in triangular ducts [13, 21, 30]. Ali and Al-Ansary [30] performed analyses on natural convection and they calculated the modified Rayleigh number values, corresponding with the transition from laminar to turbulent flow. The laminar mixed convection in horizontal triangular ducts with different apex angles was handled by Talukdar and Shah [13]. They indicated increasing Nusselt number values for increasing Rayleigh numbers and they underlined this behaviour for the duct bottom walls. A numerical investigation on nanofluid mixed convection in equilateral triangular ducts was, recently, presented by Manca et al. [21]. Walls were heated at constant temperature and Al_2O_3/water based nanofluids were considered. The improvement in terms of convective heat transfer coefficients, linked to the particle concentration and Richardson number, was accompanied by increasing values of wall shear stress.

The use of nanofluid could be encountered in the passive techniques, employing additives in fluids in order to enhance heat transfer as pointed out by Bergles [31]. Nanofluids are made up by a base fluid and suspended nanosize particles with a diameter smaller than 100 nm [32]. As a result, the thermal conductivity tends to increase according to the particle concentration. Topics related to nanofluids have become very popular to the research groups because of the possibility to improve the performances of heat exchangers or cooling devices, as reviewed recently in [33–38]. Some investigations reported promising results on heat transfer enhancement also in the case of low nanoparticle concentrations [39], although pumping power could increase dramatically, as underlined in [40]. However, a critical discussion about the results obtained by means of numerical and experimental approaches and processes, adopted by different research groups, has arisen [41–44].

This paper is concerned with the study on laminar mixed convection in triangular horizontal ducts by adopting nanofluids. One of the first papers on forced convection in equilateral triangular ducts in Al_2O_3/water nanofluids was carried out by Heris et al. [45] numerically. The walls were at constant wall temperature condition and the effects of nanoparticles diameter, concentration, and Reynolds number on the enhancement of nanofluids heat transfer were studied. The presented results indicated that Nusselt number increased decreasing the nanoparticle size and the nanoparticle concentration. A numerical investigation on mixed convective nanofluids flow and heat transfer in an isosceles triangular duct, with constant wall temperatures, was accomplished in [46]. Pure water and four different types of nanofluids (Ag, Au, eu, diamond, and SiO_2) with volume fractions range from 1% to 5% were considered. Rayleigh number was in the range 1×10^4–1×10^6 and Reynolds number ranges between 100 and 1000. The results revealed that the Nusselt number increases as Rayleigh number increases due to the buoyancy force effect. It was found that SiO_2 nanofluid presents the highest Nusselt number while Au nanofluid has the lowest Nusselt number. Moreover, an increasing of the duct apex angle decreases the Nusselt number value. The pressure drop increases as Reynolds number increases and apex angle decreases. An experimental investigation on the heat transfer of an equilateral triangular duct by employing the CuO/water nanofluid in a laminar flow and under constant heat flux condition was presented in [47]. Results showed that the experimental heat transfer coefficient of the CuO/water nanofluid is more than that of distilled water. Moreover, the measured heat transfer coefficient of a CuO/water nanofluid was greater than the theoretical one. The heat transfer enhancement of the equilateral triangular duct increased with the nanofluid volume concentration as well as the Peclet number. An investigation on laminar mixed convection in a Al_2O_3/water nanofluid, flowing in a triangular cross-sectioned duct, was numerically performed in [21]. The duct walls were at uniform temperature and the single-phase model was assumed. A fluid flow with different values of Richardson number and nanoparticle volume fractions was considered. Results showed the increase of average convective heat transfer coefficient and Nusselt number for increasing values of Richardson number and particle concentration. However, also wall shear stress and required pumping power profiles grow significantly. An experimental study to determine the pressure drop and performance characteristics of Al_2O_3/water and CuO/water nanofluids in a triangular duct under constant heat flux where the flow was laminar was performed in [48]. The results showed that, at a specified Reynolds number, using the nanofluids can lead to an increase in the pressure drop by 35%. It was also found that, with increases in the Reynolds number, the rate of increase in the friction factor with the volume fraction of nanoparticles is reduced. Moreover, a performance index (heat transfer referred to pressure drop) showed that the use of Al_2O_3/water nanofluid with volume fractions of 1.5% and 2% was not helpful in the triangular duct. It was also concluded that, at the same volume fraction of nanoparticles, using Al_2O_3 nanoparticles is more beneficial than CuO nanoparticles based on the performance index. This paper experimentally investigates the heat transfer of an equilateral triangular duct by employing an Al_2O_3/water nanofluid in laminar flow and under constant heat flux conditions was experimentally investigated in [49]. The Nusselt numbers were estimated for different nanoparticle concentrations at various Peclet numbers. The results showed that the experimental heat transfer coefficient of Al_2O_3/water nanofluid was higher than that of distillated water. Also, in this case, the experimental heat transfer coefficient of Al_2O_3/water nanofluid is higher

Downloaded from ade.sagepub.com at University of Otago Library on July 24, 2015

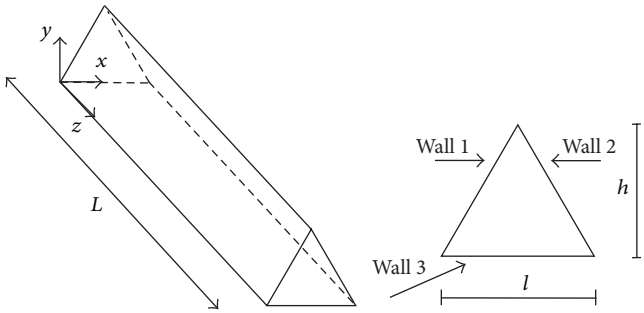

Figure 1: Sketch of the considered model.

than the theoretical one. The results pointed out that the heat transfer enhancement increases with increases in the nanofluid volume concentration and Peclet number.

The review of the literature shows that there is no study on laminar mixed convection in equilateral triangular ducts in nanofluids, with the wall at uniform heat flux.

In this paper, results obtained by the numerical investigation on laminar mixed convection in triangular ducts, filled with nanofluids, are presented in order to evaluate the fluid dynamic and thermal features of the considered geometry by considering Al_2O_3/water based nanofluids. The system is heated by a constant and uniform heat flux also along the perimeter of the triangular duct section (H2 mode, thermal boundary condition) and the single-phase model has been assigned for a Reynolds number value equal to 100. Results are given for different nanoparticle volume concentrations and Richardson number values ranging from 0% to 5% and 0 to 5, respectively.

2. Geometrical Configuration and Governing Equations

A duct with an equilateral triangular cross-section, triangular duct, is investigated and the geometrical configuration is shown in Figure 1. The triangular duct with the length L, equal to 2.00 m, is heated on the walls at a constant and uniform heat flux also along the perimeter of the triangular duct section (H2 mode, thermal boundary condition). The channel edge length, l, is 0.0170 m and the hydraulic diameter, defined by $D_h = 4A/P_h$, is equal to 0.0100 m. The working fluid is a nanofluid which is composed of water and Al_2O_3 nanoparticles.

The flow in the duct is assumed to be three-dimensional, steady-state, laminar, and incompressible with negligible viscous dissipation. Thermophysical properties of the nanofluid are considered constant with temperature, except for the dependence of density on the temperature, Boussinesq approximation, which determines the buoyancy force. The single-phase model is assumed and the governing equations under the aforementioned assumptions are in a Cartesian rectangular coordinate system [21, 50]:

$$\begin{aligned}
\text{Continuity: } & \frac{\partial u}{\partial x} + \frac{\partial v}{\partial y} + \frac{\partial w}{\partial z} = 0 \\
\text{Momentum: } & \left[u\frac{\partial u}{\partial x} + v\frac{\partial u}{\partial y} + w\frac{\partial u}{\partial z}\right] \\
& = -\frac{1}{\rho}\frac{\partial P}{\partial x} + \nu\left[\frac{\partial^2 u}{\partial x^2} + \frac{\partial^2 u}{\partial y^2} + \frac{\partial^2 u}{\partial z^2}\right], \\
& \left[u\frac{\partial v}{\partial x} + v\frac{\partial v}{\partial y} + w\frac{\partial v}{\partial z}\right] \\
& = -\frac{1}{\rho}\frac{\partial P}{\partial y} + \nu\left[\frac{\partial^2 v}{\partial x^2} + \frac{\partial^2 v}{\partial y^2} + \frac{\partial^2 v}{\partial z^2}\right] \\
& \quad + \beta g\left(T - T_{\text{in}}\right), \\
& \left[u\frac{\partial w}{\partial x} + v\frac{\partial w}{\partial y} + w\frac{\partial w}{\partial z}\right] \\
& = -\frac{1}{\rho}\frac{\partial P}{\partial z} + \nu\left[\frac{\partial^2 w}{\partial x^2} + \frac{\partial^2 w}{\partial y^2} + \frac{\partial^2 w}{\partial z^2}\right], \\
\text{Energy: } & \left[u\frac{\partial T}{\partial x} + v\frac{\partial T}{\partial y} + w\frac{\partial T}{\partial z}\right] \\
& = \lambda\left[\frac{\partial^2 T}{\partial x^2} + \frac{\partial^2 T}{\partial y^2} + \frac{\partial^2 T}{\partial z^2}\right].
\end{aligned} \tag{1}$$

At the end of the duct, a fully developed flow is considered; the following boundary conditions are assumed:

(i) inlet section: uniform velocity and temperature profile;

(ii) outlet section: outflow condition with velocity components and temperature derivatives equal to zero;

(iii) duct walls: velocity components equal to zero and assigned uniform and constant heat flux.

The considered dimensionless characteristic numbers are the Reynolds number, the Grashof number, the Richardson number, the Nusselt number, and the friction factor for the data reduction. They are expressed by the following relations:

$$\text{Re} = \frac{V d_h}{\nu}, \tag{2}$$

$$\text{Gr} = \frac{g\beta\dot{q} {d_h}^4}{\lambda\nu^2}, \tag{3}$$

$$\text{Ri} = \frac{\text{Gr}}{\text{Re}^2}, \tag{4}$$

$$\text{Nu}_{\text{av}} = \frac{\dot{q} d_h}{\left(T_w - T_m\right)\lambda_f}, \tag{5}$$

$$f = 2\Delta P\frac{d_h}{L}\frac{1}{\rho V^2}, \tag{6}$$

where V is the average inlet velocity, $\dot{q}$ is the heat flux, and T_w and T_m represent the wall and the bulk fluid temperatures, respectively.

Downloaded from ade.sagepub.com at University of Otago Library on July 24, 2015

Table 1: Material properties at the reference temperature of 293 K, given by [29].

Material	ρ [kg/m^3]	c_p [J/kg K]	β [1/K]	μ [Pa s]	λ [W/mK]
Al_2O_3	3880	773	//	//	36
Water	998.2	4128	$2.100e^{-4}$	$993e^{-6}$	0.597

Table 2: Thermophysical properties of the working fluids.

ϕ	ρ [kg/m^3]	c_p [J/kg K]	β [1/K]	μ [Pa s]	λ [W/mK]
0%	998.2	4182	$2.100e^{-4}$	$993e^{-6}$	0.597
1%	1027	4053	$2.098e^{-4}$	$1082e^{-6}$	0.622
2%	1056	3931	$2.095e^{-4}$	$1193e^{-6}$	0.636
3%	1085	3816	$2.093e^{-4}$	$1233e^{-6}$	0.648
4%	1113	3707	$2.090e^{-4}$	$1511e^{-6}$	0.658
5%	1143	3603	$2.090e^{-4}$	$1747e^{-6}$	0.668

3. Thermophysical Properties of Nanofluids

The considered working fluid was pure water or Al_2O_3/water based nanofluids with a particle diameter of 30 nm. The single-phase model approach was adopted in order to describe the nanofluid behavior because small temperature differences and small particle volume fractions were considered. In Table 1, the values of density, specific heat, dynamic viscosity, and thermal conductivity, given by Rohsenow et al. [51], are reported for water and Al_2O_3 particles at the reference temperature of 293 K. Nanofluids are featured by volume concentrations, equal to 1%, 2%, 3%, 4%, and 5%, which influence the properties of the working fluid. Thus, the thermophysical properties must be evaluated by employing equations, available in literature [21, 52–56]. They are reported in Table 2 and they are constant with temperature. The reference temperature at which thermal properties were evaluated was equal to 293 K. Density was evaluated by using the classical formula valid for conventional solid-liquid mixtures while the specific heat values and thermal expansion coefficient ones were calculated by assuming the thermal equilibrium between nanoparticles and surrounding fluid [21, 52–54]. The thermal expansion coefficient values were evaluated by adopting the relation given in [26] for different volume particle concentrations:

$$\text{Density: } \rho_{nf} = (1-\phi)\,\rho_{bf} + \phi\rho_p,$$

$$\text{Specific heat: } \left(\rho c_p\right)_{nf} = (1-\phi)\left(\rho c_p\right)_{bf} + \phi\left(\rho c_p\right)_p,$$

$$\text{Thermal expansion coefficient: } \frac{\beta_{nf}}{\beta_{bf}} = \frac{1}{\left(\left((1-\phi)/\phi\right)\left(\rho_{bf}/\rho_p\right)\right)}\frac{\beta_p}{\beta_{bf}} + \frac{1}{\left(\left(\phi/(1-\phi)\right)\left(\rho_{bf}/\rho_p\right)+1\right)}. \quad (7)$$

Viscosity and thermal conductivity were evaluated by means of the equations, given by [56], which were adopted because they are expressed as a function of particle volume concentration and diameter:

$$\text{Dynamic viscosity: } \frac{\mu_{nf}}{\mu_{bf}} = \frac{1}{1-34.87\left(d_p/d_f\right)^{-0.3}\phi^{1.03}} \quad (8)$$

with $d_f = 0.1(6M/N\pi\rho_{f,0})$, in which M is the molecular weight of the base fluid, N is the Avogadro number, and $\rho_{f,0}$ is the mass density of the base fluid calculated at $T = 293$ K.

Consider

$$\text{Thermal conductivity: } \frac{\lambda_{nf}}{\lambda_{bf}} = 1 + 4.4\mathrm{Re}^{0.4}\mathrm{Pr}^{0.66}\left(\frac{T}{T_{fr}}\right)^{10}\cdot\left(\frac{\lambda_p}{\lambda_{bf}}\right)^{0.03}\phi^{0.66} \quad (9)$$

with $\mathrm{Re} = 2\rho_{bf}k_bT/\pi{\mu_{bf}}^2 d_p$, in which k_b is the Boltzmann constant, equal to 1.36×10^{-26}, and T_{fr} is equal to 273.15 K.

4. Numerical Model

The governing equation (1) with the assumed boundary conditions was solved by means of Fluent code [57]. A segregated method was chosen to solve the stationary equations and a second-order upwind scheme was employed for energy and momentum equations. Pressure and velocity were coupled by using SIMPLE coupling scheme. Simulations were considered converged by assuming the convergence criteria of 10^{-4} and 10^{-5} and 10^{-8} for the residuals of continuity, velocity components, and energy, respectively. At the inlet section, flow was considered laminar, with a velocity corresponding to Reynolds number equal to 100, at a temperature of 293 K and ambient pressure conditions. The no-slip condition was applied on the channels walls, which were heated by a uniform and constant heat flux. Different values of Grashof number, ranging from 0 to 50000, were considered.

The grid-independence analysis has been performed by testing four different mesh distributions. Pure water, flowing at Re = 100, was assumed as working fluid. The considered grid configurations had 152190, 302778, 563104, and 1146232 nodes, respectively. The third grid was adopted in order to run the simulations because it leads to a good compromise between the computational time and the accuracy requirements. In fact, the comparison with the fourth configuration for pure water shows differences of 0.74% and 0.32% at most in terms of average Nusselt number and pressure coefficient. Validation has been accomplished by comparing the results at Re = 100 and Ri = 0 with literature data for H_1 boundary conditions, thermal boundary condition referring to constant axial wall heat flux with constant peripheral wall temperature [25]. In particular, the comparison in terms of local and average Nusselt number has been accomplished by considering data obtained by Wilbulswas [29] and also reported in [25]. Data are presented as a function of the axial

Downloaded from ade.sagepub.com at University of Otago Library on July 24, 2015

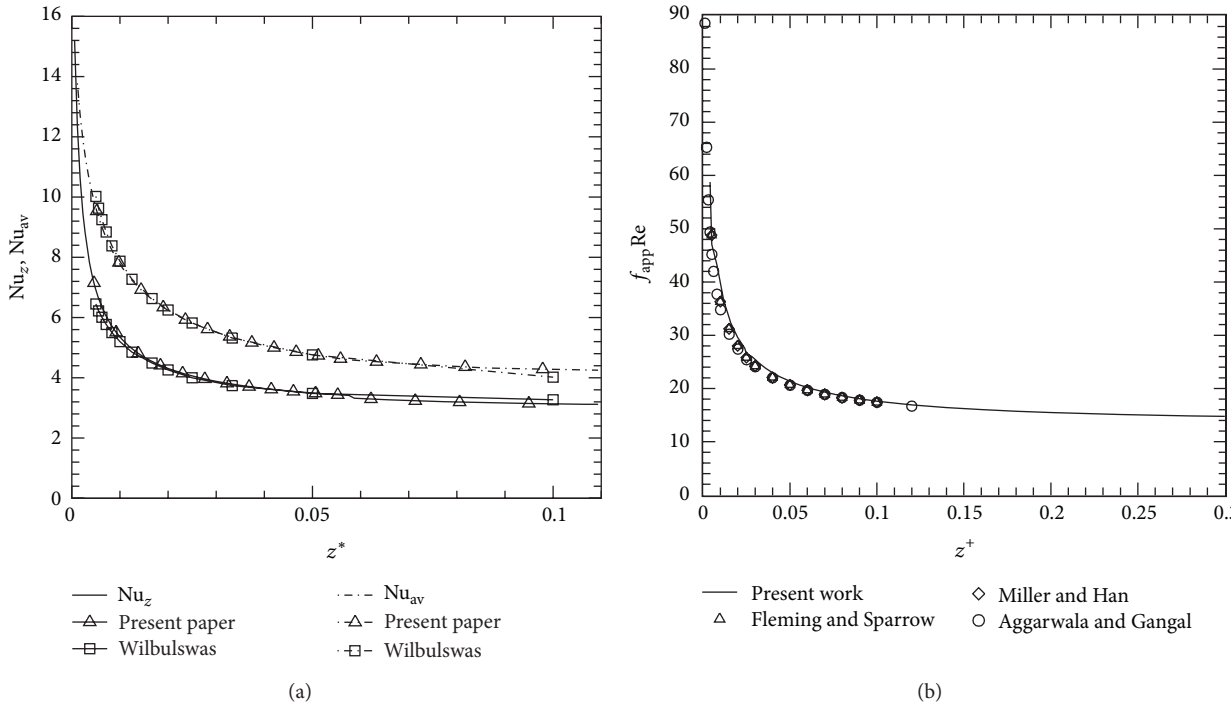

FIGURE 2: Validation of results, pure water at Re = 100 and Ri = 0: (a) average and local Nusselt number; (b) friction factor.

coordinate for the thermal entrance region, z^*, defined as $z^* = z/(d_h \mathrm{Re})$. Furthermore, the validation in terms of friction factor has been performed by comparing data from Fleming and Sparrow [58], Miller and Han [59], and Aggarwala and Gangal [26], also reported in [25], with the obtained results for fully developed laminar flow in forced convection. Data reduction has been performed by considering the axial coordinate for the hydrodynamic entrance region, such as z^+ parameter, defined by $z^* = z/(d_h \mathrm{Pe})$. Figure 2 shows these comparisons and it is clear that the present numerical results are in good agreement with the literature data. In particular, a maximum difference of 3% is observed for local and average Nusselt number at most, as shown in Figure 2(a), while a maximum error of 1% is evaluated in terms of friction factor, as reported in Figure 2(b).

5. Results and Discussion

Results of the numerical simulation are presented and discussed. They are carried out for a Reynolds number, Re, value equal to 100, Richardson number, Ri, ranging from 0.0 to 5.0, and the nanoparticle volume fractions, ϕ, in the 0%–5.0% range.

Results are reported in terms of average convective heat transfer coefficient, average Nusselt number, wall shear stress, required pumping power profiles, and temperature and velocity distributions at particular channel sections.

The average convective heat transfer coefficient profiles as a function of Ri number values for different nanoparticle volume fractions are shown in Figure 3(a). It is observed that the heat transfer coefficient increases as the effects of buoyancy tend to become more intense for higher Ri numbers. Furthermore, a very sharp increase in profiles is noted at small values of Ri number. In the case of pure water, such as at $\phi = 0\%$, h_{avg} is equal to about 114, 142, 184, 203, 222, 233, and 245 $\mathrm{W/m^2\,K}$ for Ri = 0, 0.1, 0.5, 1, 2, 3, and 5, respectively. When nanofluids replace pure water as working fluids, it is still important to pay attention to the buoyancy effects in order to evaluate the thermal performances of the duct. Moreover, nanoparticle concentrations change the thermophysical properties of working fluids and improve the thermal conductivity. As a result, the average heat transfer coefficients increase. In fact, h_{avg} is equal to about 120, 148, 191, 212, 231, 242, and 256 $\mathrm{W/m^2\,K}$ at $\phi = 1\%$ while at $\phi = 5\%$ h_{avg} is equal to about 128, 165, 212, 233, 254, 266, and 279 $\mathrm{W/m^2\,K}$ for Ri = 0, 0.1, 0.5, 1, 2, 3, and 5, respectively. Figure 3(b) compares the enhancement in terms of convective heat transfer with the configurations considering pure water for Ri = 0. The highest enhancement is obviously evaluated for $\phi = 5\%$ and heat transfer coefficient values are 1.44, 2.03, 2.21, and 2.43 times greater than the ones obtained for the reference case, for Ri = 0.1, 1, 2, and 5, respectively. However, an average increase of 16% is calculated comparing results obtained for $\phi = 5\%$ with ones evaluated for $\phi = 0\%$, at a fixed Ri number value.

The average Nusselt profiles, as a function of Ri, for different values of nanoparticle volume concentrations are depicted in Figure 4(a). For fully developed laminar flow in forced convection, such as at Ri = 0, Nusselt number is equal to 1.9 for triangular ducts under the hypothesis of H_2 boundary conditions, applied on the duct walls. As observed for the convective heat transfer profiles, average Nusselt

Downloaded from ade.sagepub.com at University of Otago Library on July 24, 2015

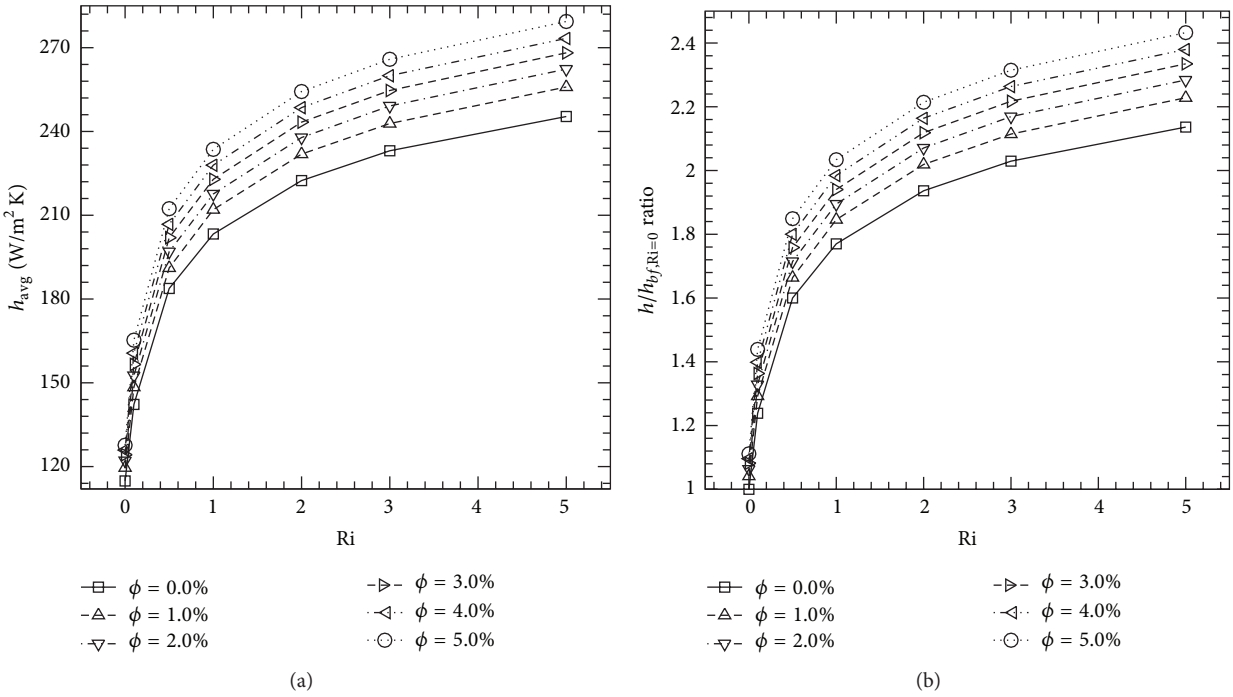

FIGURE 3: Convective heat transfer coefficient profiles as a function of Ri, ϕ = 0%, 1%, 2%, 3%, 4%, and 5%: (a) average convective heat transfer coefficient; (b) average convective heat transfer coefficient enhancement, referred to pure water case at Ri = 0.

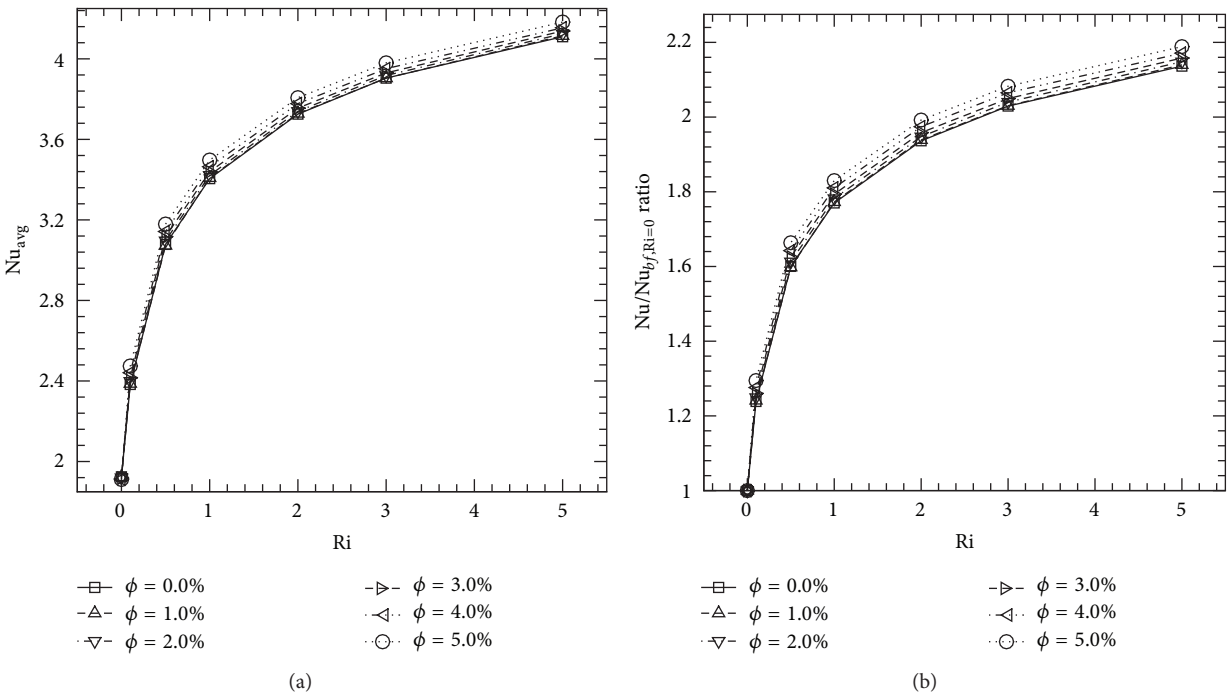

FIGURE 4: Nusselt number profiles as a function of Ri, ϕ = 0%, 1%, 2%, 3%, 4%, and 5%: (a) average Nusselt number values; (b) average Nusselt number enhancement, referred to pure water case at Ri = 0.

Downloaded from ade.sagepub.com at University of Otago Library on July 24, 2015

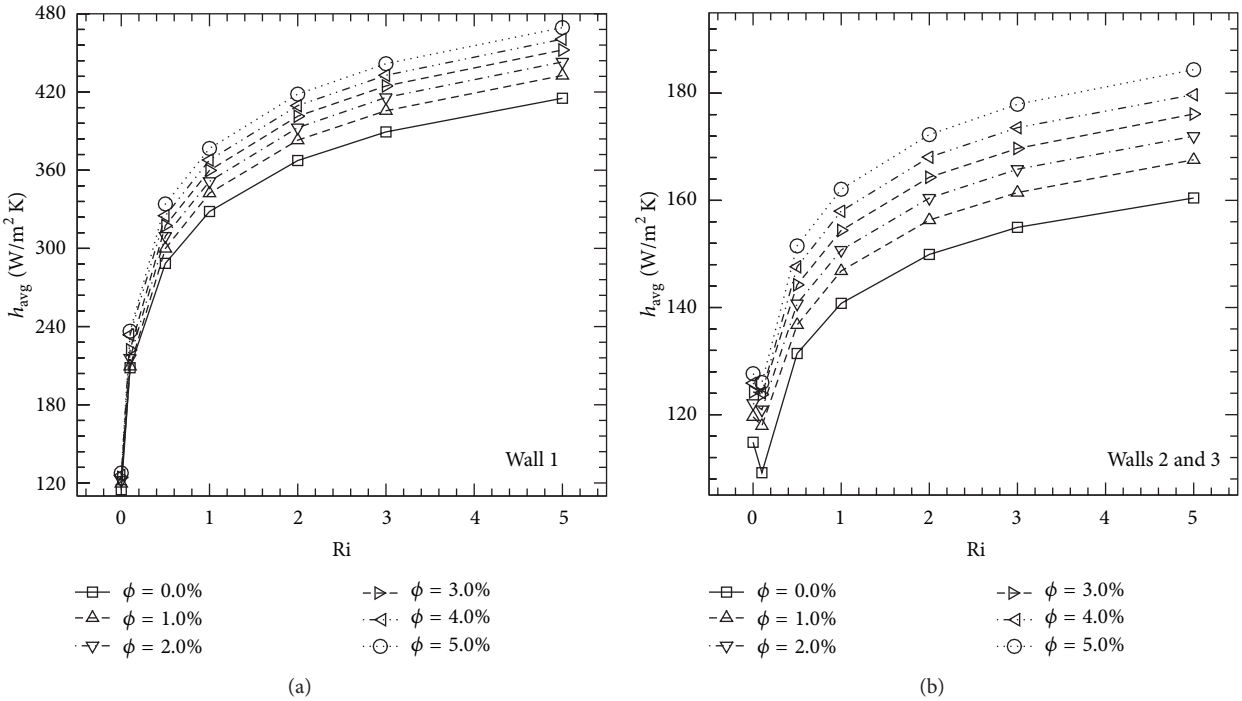

FIGURE 5: Average convective heat transfer coefficient profiles as a function of Ri, ϕ = 0%, 1%, 2%, 3%, 4%, and 5%: (a) wall 1; (b) walls 2 and 3.

number tends to increase in the test section for increasing Ri number values. Moreover, nanoparticle fraction growth leads to a slight increase of Nu_{avg} values. In fact, for Ri = 1, Nu_{avg} is equal to 3.37, 3.41, 3.42, 3.44, 3.46, and 3.51 at ϕ = 0%, 1%, 2%, 3%, 4%, and 5%. The enhancement in terms of average Nusselt number is presented in Figure 4(b); it is clear that the increase of Nusselt number, compared to the value calculated for the forced convection in pure water, is less significant if compared with the profiles evaluated for the convective heat transfer coefficients because the nanofluid thermal conductivity increases according to the particle concentration. In fact, for ϕ equal to 1% and 5%, the average Nusselt number is 2.14 and 2.20 times the values detected for Ri = 0 in pure water. Values of 1% and % 4% higher than the cases with pure water on average at a fixed value of Ri were calculated.

Heat transfer mechanisms in ducts, having triangular shaped cross-sections, in the case of laminar mixed convection are obviously linked to the effects of buoyancy. In fact, different behaviours are detected for the inclined heated walls and the bottom one, respectively. On the other hand, for Ri = 0, no differences are evaluated if the three walls are compared but when buoyancy is taken into account, for example, heat transfer coefficients are higher for the bottom wall, according to Ri number. Figure 5 helps to describe these behaviours. The convective heat transfer profiles for the bottom wall are reported in Figure 5(a). The increase of h_{avg} for increasing Ri number values was observed, as expected. In the case of pure water, h_{avg} values of wall 1 are equal to about 113, 208, 289, 328, 367, 389, and 415 W/m^2 K for Ri = 0, 0.1, 0.5, 1, 2, 3, 4, and 5, respectively. Moreover, increasing values of nanoparticle volume concentration lead to a significant enhancement of heat transfer coefficients even at low Ri numbers. For ϕ = 5%, the highest heat transfer coefficient value is detected for Ri = 5 and it is equal to about 472 W/m^2 K. The average heat transfer coefficient values are equal to about 127, 236, 334, 376, 418, and 441 W/m^2 K for Ri = 0, 0.1, 0.5, 1, 2, 3, and 4. For the inclined walls, such as wall 2 and wall 3, smaller values of h_{avg} than the ones observed for wall 1 are evaluated, as reported in Figure 5(b). In fact, at Ri = 1, h_{avg} is equal to 140, 147, 150, 154, 158, and 162 W/m^2 K for ϕ = 0%, 1%, 2%, 3%, 4%, and 5%, respectively, while for Ri = 5 h_{avg} is equal to about 160, 168, 172, 176, 180, and 184 W/m^2 K. Furthermore, for Ri = 0.1, buoyancy determines negative effects on the heat transfer mechanism if results are compared with ones obtained in the case of forced convection. In fact, minimum values of 109, 118, 121, 123, 124, and 126 W/m^2 K are detected for ϕ = 0%, 1%, 2%, 3%, 4%, and 5%, respectively.

The employment of nanofluids leads generally to an increase of wall shear stress and pumping power in order to provide the described heat transfer enhancement in comparison with pure fluids. Figure 6 shows the wall shear stress profiles in order to underline the disadvantages of nanofluid employment. The average wall shear stress profiles as a function of Ri are reported in Figure 6; they increase as the buoyancy effects become more important and the highest values are evaluated at Ri = 5. The increase of nanoparticle concentration leads to a significant increase in terms of wall shear stress: the highest values are evaluated for ϕ = 5%. The comparison with the wall shear stress values, calculated

Downloaded from ade.sagepub.com at University of Otago Library on July 24, 2015

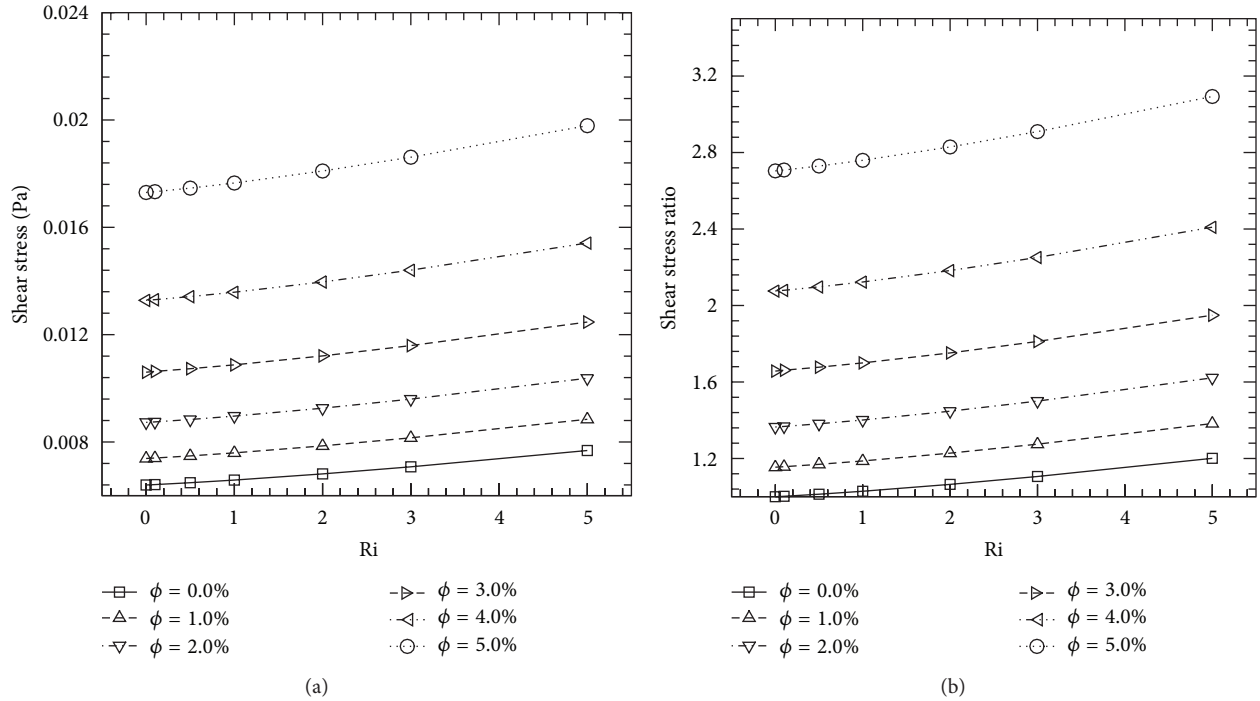

FIGURE 6: Wall shear stress profiles as a function of Ri, ϕ = 0%, 1%, 2%, 3%, 4%, and 5%: (a) average wall shear stress; (b) average wall shear stress, referred to the pure water case at Ri = 0.

for pure water at Ri = 0, is reported in Figure 6(b). It is shown that wall shear stress ratio is equal to about 2.70, 2.73, 2.76, 2.82, and 3.09 at ϕ = 5% for Ri = 0, 0.5, 1, 2, and 5. For lower nanoparticle concentrations, wall shear stress ratio tends to decrease and, for example, it is equal to about 1.15, 1.17, 1.19, 1.23, and 1.38 for ϕ = 1% and Ri = 0, 0.5, 1, 2, and 5, respectively.

Wall shear stress profiles change if the inclined walls are compared with the bottom one. In fact, wall 1 shows higher average wall shear stress values than the ones obtained for wall 2 and wall 3, as depicted by Figure 7. Furthermore, Figure 7(a) reports increasing profiles as Ri number values grow. Increasing particle concentrations lead to increasing values of wall shear stress. Wall 2 and wall 3 are featured by substantially constant values of wall shear stress, as observed in Figure 7(b).

Figure 8 shows the dimensionless temperature distributions for two values of Ri number, such as 1 and 3, in correspondence with the vertical symmetry axis at z/d_h = 125 and 150. The dimensionless temperature is defined by $T^* = (T_m - T)/(\dot{q}d_h/\lambda)$; the maximum values are evaluated at y/h equal to about 0.87 and negative values are evaluated near the walls, which are featured by higher temperature values than the fluid ones. Figure 9 describes the fully developed flow regime in terms of velocity profiles in correspondence with the vertical symmetry axis of the duct at two sections, z/d_h = 125 and 150, for Ri = 1 and 3. Profiles of $u/u_{\max}$ substantially overlap each other for different values of particle concentration values and Richardson number. The maximum velocity is evaluated at y/h equal to about 0.72 for all the considered values of ϕ and Ri.

The required pumping power profiles are reported in Figure 10(a). Pumping power is defined as PP = $\dot{V}\Delta P$. It is shown that profiles are slightly dependent on Ri number but a clear influence of particle concentrations on results is observed. In fact, the pressure drop, ΔP, is strongly related to the shear stress and the increase in volumetric concentration determines a significant pumping power increase, as indicated in Figure 10(a). Results, compared to the water cases at Ri = 0, are presented in Figure 10(b) where the pumping power ratio is reported. It is equal to about 1.22, 1.55, 2.05, 2.83, and 4.16, at Ri = 0 and 1.26, 1.59, 2.10, 2.90, and 4.25, at Ri = 5, for ϕ = 1%, 2%, 3%, 4%, and 5%, respectively. The values confirm that the pumping power has a slight dependence on Richardson number.

The advantage in the use of nanofluids can be suggested by employing the performance evaluation criterion (PEC). It can be defined as in [60]:

$$\text{PEC} = \frac{Q}{\text{PP}} \tag{10}$$

with Q as the heat transfer rate exchanged between the wall of the duct and the working fluid and as PP the pumping power to move the working fluid inside the duct. However, for assigned wall heat flux thermal boundary conditions, (10) provides always a PEC value less than 1 because the heat transfer rate is constant for all ϕ and Ri values whereas PP increases, significantly, with ϕ. In this case, the PEC should be defined as in [1]:

$$\text{PEC} = \frac{\text{Nu}_{nf}/\text{Nu}_{bf}}{\left(f_{nf}/f_{bf}\right)^{1/3}}. \tag{11}$$

Downloaded from ade.sagepub.com at University of Otago Library on July 24, 2015

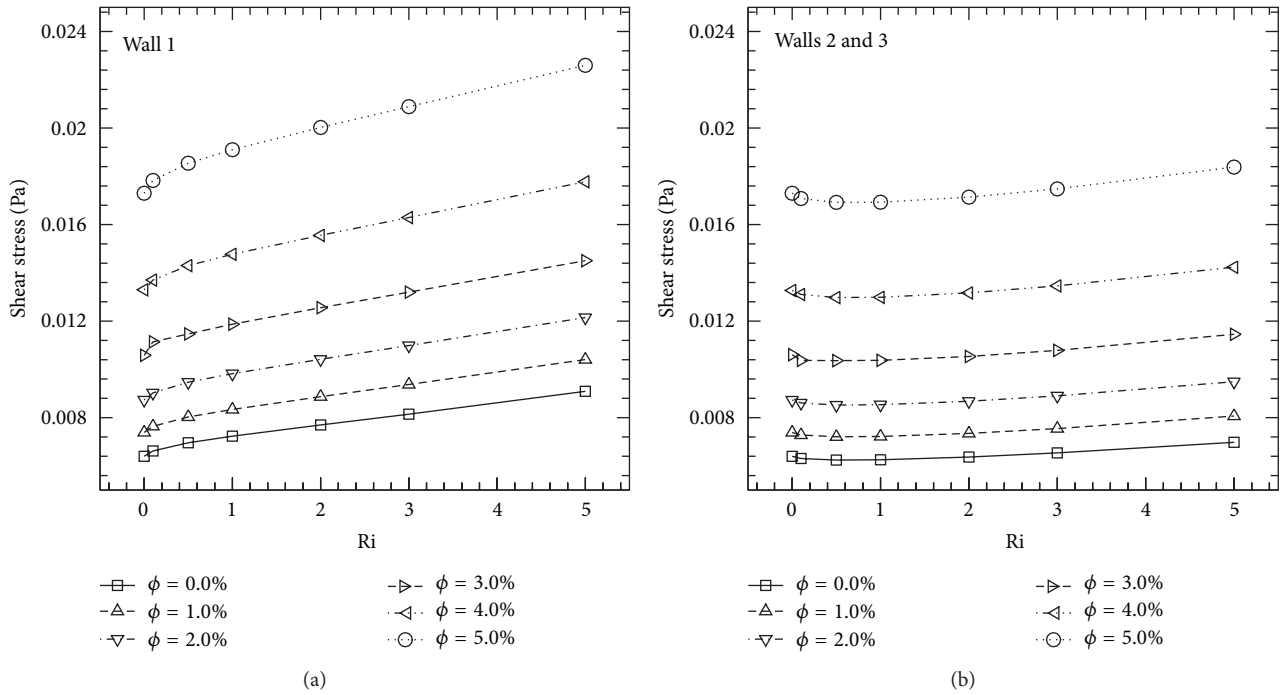

FIGURE 7: Average wall shear stress profiles as a function of Ri, ϕ = 0%, 1%, 2%, 3%, 4%, and 5%: (a) wall 1; (b) walls 2 and 3.

The ratio f_{nf}/f_{bf} is about 1 [21] and the PEC is about equal to the ratio $\mathrm{Nu}_{nf}/\mathrm{Nu}_{bf}$. As a consequence, it results that the use of nanofluids in mixed convection seems slightly convenient as is shown in Figure 4(b). It is noted that the maximum increase is obtained for ϕ = 5% and the corresponding percentage increase, referred to the value for base fluid, is not greater than 5%.

The average Nusselt number is correlated with the Richardson number and particle volume concentration. Two equations are given for ϕ = 0%, for Ri numbers ranging from 0 to 5, and ϕ = 1%, 2%, 3%, 4%, and 5%, for Ri in the range 0.1–5, respectively. Least-squares curve fittings of the obtained numerical data have the following correlation forms:

$$\mathrm{Nu}_{\mathrm{avg}} = a + b\mathrm{Ri}^{c},$$
$$\mathrm{Nu}_{\mathrm{avg}} = a\mathrm{Ri}^{b}\phi^{c}. \tag{12}$$

In particular, correlations have a 1.5% and 1.62% estimated standard deviation, respectively. The following equations are proposed:

$$\mathrm{Nu}_{\mathrm{avg}} = 1.88 + 1.423\mathrm{Ri}^{0.3097},$$
$$\mathrm{Nu}_{\mathrm{avg}} = 3.5726\mathrm{Ri}^{0.1381}\phi^{0.0146}. \tag{13}$$

The regression coefficient, R^2, of (13) is equal to 0.9936 and 0.9927 and correlations are plotted in Figures 11(a) and 11(b).

6. Conclusions

Results about the numerical analysis on laminar mixed convection with nanofluids flowing in triangular cross-sectioned ducts are presented in this paper. Walls are heated at uniform and constant heat flux, depending on Richardson number and Al_2O_3/water based nanofluids at volume concentrations equal to 0%, 1%, 2%, 3%, 4%, and 5% were considered. Reynolds number was set to 100 while Richardson numbers ranged from 0 to 5. The single-phase model was adopted in order to describe the behaviour of nanofluids as working fluids and thermophysical properties were evaluated by means of equations, available in literature.

The simulations result showed the increase of the convective heat transfer coefficients, in particular, for high concentration of nanoparticles and for increasing values of Richardson number. The highest enhancement is evaluated for ϕ = 5% with the average convective heat transfer coefficient values equal to 1.44, 2.03, 2.21, and 2.43 times greater than the ones obtained for the reference case, at Ri = 0.1, 1, 2, and 5, respectively. However, the disadvantages are represented by the growth of the wall shear stress and the required pumping power, observed in particular at high particle concentrations. The pumping power ratio, referred to the pure water cases in forced convection, is equal to 1.26, 1.59, 2.10, 2.90, and 4.25 for ϕ = 1%, 2%, 3%, 4%, and 5% at most, respectively.

It should be underlined that, at moment, experimental data are not available to compare the numerical proposed model for mixed convection in horizontal triangular ducts with nanofluids. It is important to have in the future some experimental investigation related to the mixed convection in horizontal triangular ducts with nanofluids in order to

Downloaded from ade.sagepub.com at University of Otago Library on July 24, 2015

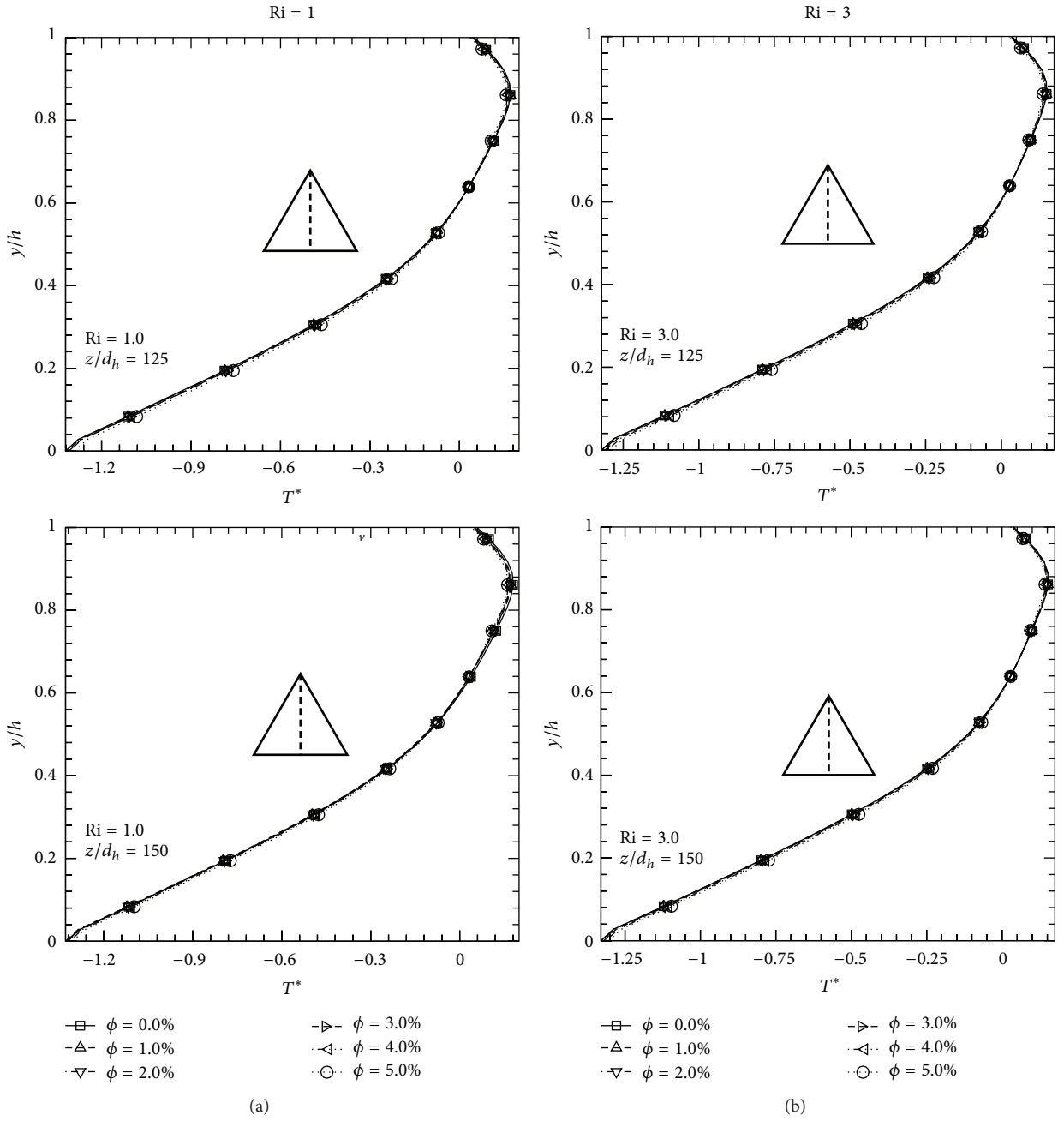

FIGURE 8: Dimensionless temperature distributions for different values of particle concentration and Ri = 1 and 3 in correspondence with the vertical symmetry axis: (a) $z/d_h = 125$; (b) $z/d_h = 150$.

evaluate the possible goodness of the numerical model related to the proposed results presented here.

Nomenclature

A: Cross-section area (m^2)
c_p: Specific heat (J/kgK)
d: Duct diameter (m)
f: Friction factor (see (6))
g: Gravitational acceleration (m/s^2)
Gr: Grashof number (see (3))
h: Heat transfer coefficient (W/m^2K)
H: Duct height (m)
l: Duct edge length (m)
L: Total duct length (m)
Nu: Nusselt number (see (5))
P: Pressure (Pa)
Pe: Peclet number
PP: Pumping power (W)
Pr = ν/a: Prandtl number
q: Heat flux (W/m^2)
Re: Reynolds number (see (2))

Downloaded from ade.sagepub.com at University of Otago Library on July 24, 2015

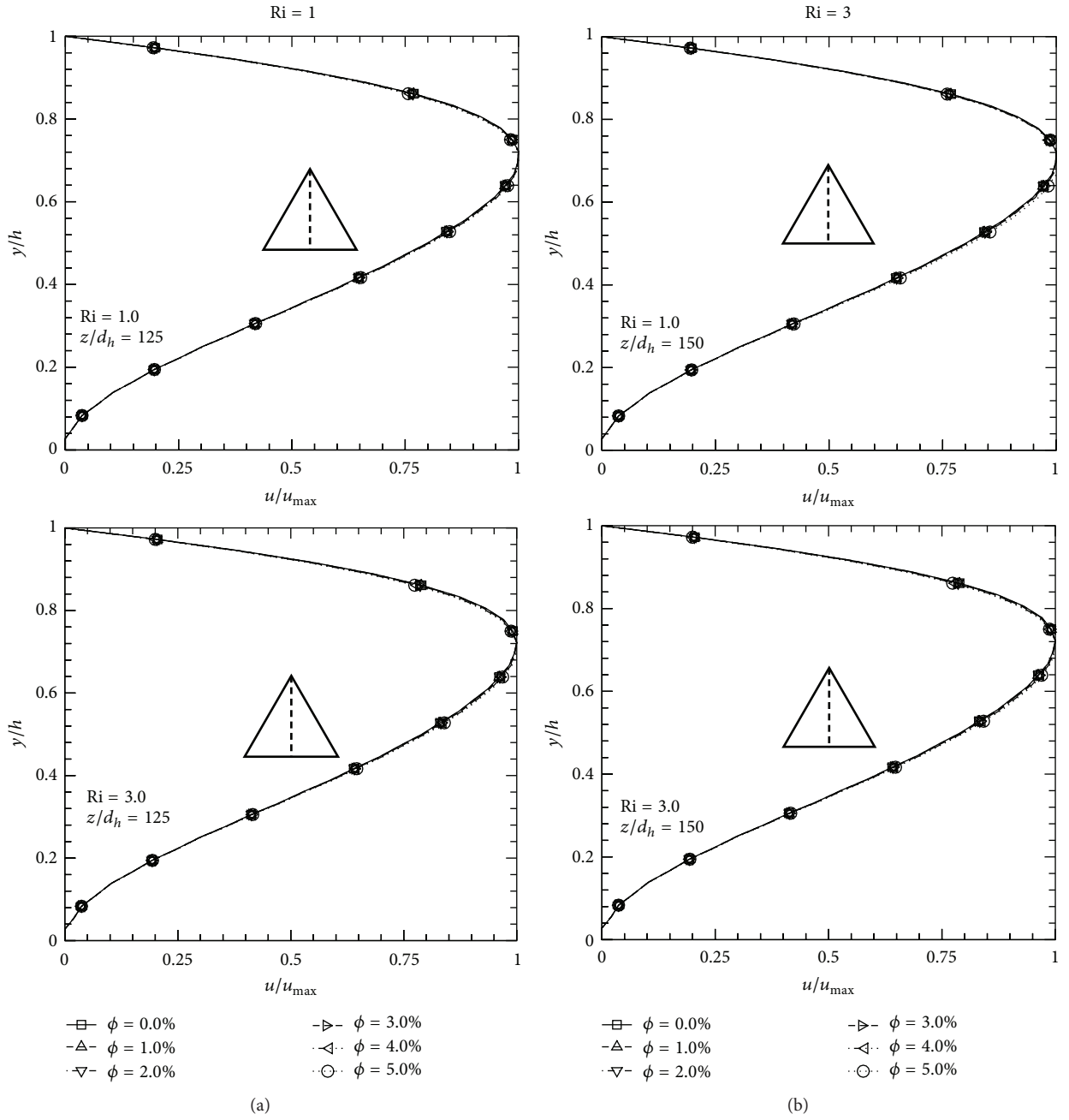

FIGURE 9: Velocity profiles for different values of particle concentration and Ri = 1 and 3 in correspondence with the vertical symmetry axis: (a) $z/d_h = 125$; (b) $z/d_h = 150$.

Ri: Richardson number (see (4))
T: Temperature (K)
u, v, w: Velocity component (m/s)
V: Average velocity (m/s)
$\dot{V}$: Volume flow rate (m^3/s)
x, y, z: Spatial coordinates (m).

Greek Symbols

α: Thermal diffusivity (m^2/s)
β: Volumetric expansion coefficient (1/K)
λ: Thermal conductivity (W/m K)
μ: Dynamic viscosity (Pa s)
ρ: Density (kg/m^3)
τ: Wall shear stress (kg/m)
ν: Kinematic viscosity (m^2/s)
ϕ: Nanoparticle volumetric concentration.

Subscripts

avg: Average
b_f: Base fluid

Downloaded from ade.sagepub.com at University of Otago Library on July 24, 2015

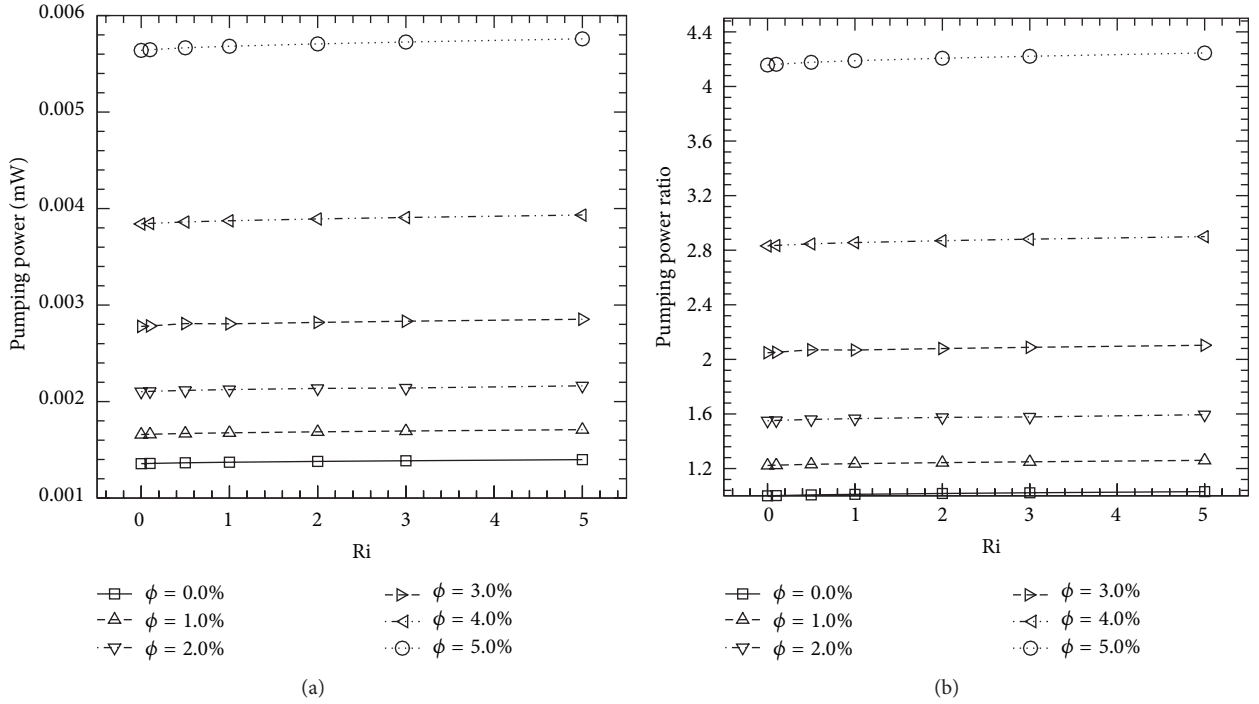

FIGURE 10: Required pumping power profiles as a function of Ri, ϕ = 0%, 1%, 2%, 3%, 4%, and 5%: (a) pumping power; (b) pumping power, referred to the pure water case at Ri = 0.

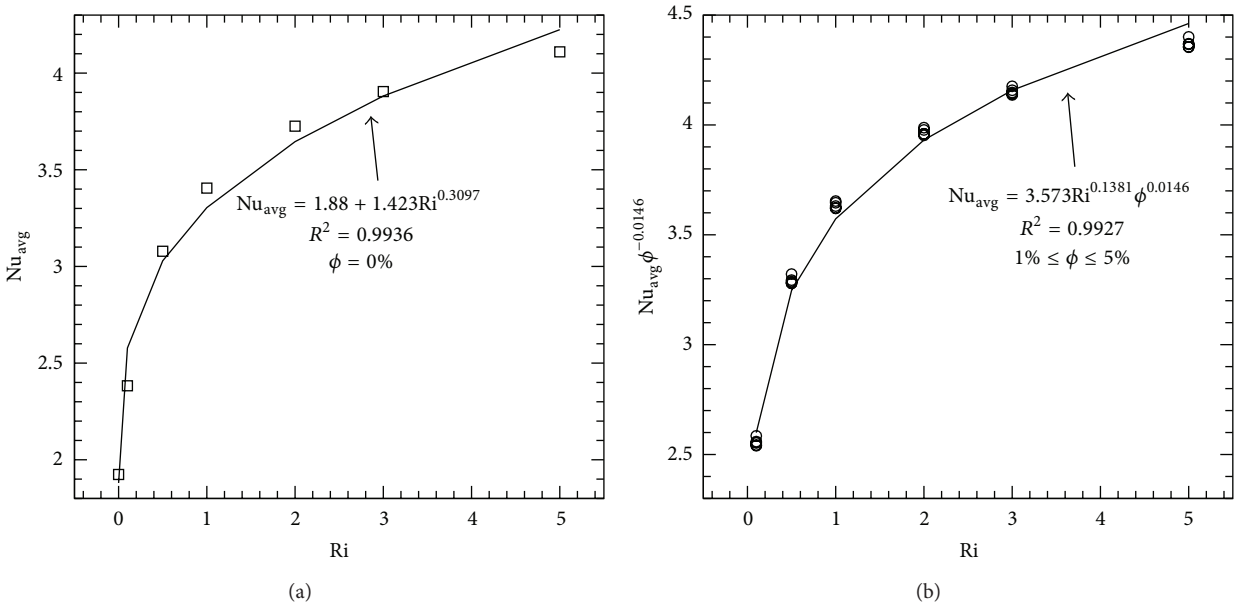

FIGURE 11: Proposed correlations for average Nusselt number: (a) correlations as a function of Ri, in the range 0–5, pure water cases; (b) correlations as a function of Ri, in the range 0.1–5, and ϕ = 1%, 2%, 3%, 4%, and 5%.

Downloaded from ade.sagepub.com at University of Otago Library on July 24, 2015

f: Fluid
h: Hydraulic
m: Mass
n_f: Nanofluid
p: Solid particle
w: Wall.

Conflict of Interests

The authors declare that there is no conflict of interests regarding the publication of this paper.

Acknowledgments

This work was supported by SUN with a 2010 grant and by MIUR with Articolo D.M. 593/2000 Grandi Laboratori "EliosLab." This work was financially supported by the Italian Government, MIUR Grant PRIN-2009KSSKL3.

References

[1] R. L. Webb and N. H. Kim, *Principles of Enhanced Heat Transfer*, Taylor & Francis, New York, NY, USA, 2nd edition, 2005.

[2] S. R. Montgomery and P. Wibulswas, "Laminar flow heat transfer ducts of rectangular cross-section," in *Proceedings of the 3rd International Heat Transfer Conference*, pp. 85–96, New York, NY, USA, 1966.

[3] R. K. Shah, "Laminar flow friction and forced convection heat transfer in ducts of arbitrary geometry," *International Journal of Heat and Mass Transfer*, vol. 18, no. 7-8, pp. 849–862, 1975.

[4] Y. Asako and M. Faghri, "Three-dimensional laminar heat transfer and fluid flow characteristics in the entrance region of a rhombic duct," *Journal of Heat Transfer*, vol. 110, no. 4, pp. 855–861, 1988.

[5] K. Velusamy, V. K. Garg, and G. Vaidyanathan, "Fully developed flow and heat transfer in semi-elliptical ducts," *International Journal of Heat and Fluid Flow*, vol. 16, no. 2, pp. 145–152, 1995.

[6] I. Uzun and M. Unsal, "A numerical study of laminar heat convection in ducts of irregular cross-sections," *International Communications in Heat and Mass Transfer*, vol. 24, no. 6, pp. 835–848, 1997.

[7] R. Gupta, P. E. Geyer, D. F. Fletcher, and B. S. Haynes, "Thermo-hydraulic performance of a periodic trapezoidal channel with a triangular cross-section," *International Journal of Heat and Mass Transfer*, vol. 51, no. 11-12, pp. 2925–2929, 2008.

[8] N. Jesuthasan and B. R. Baliga, "A Numerical method for three-dimensional parabolic flow and heat transfer in straight ducts of irregular cross section," *Computational Thermal Sciences*, vol. 1, no. 3, pp. 259–288, 2009.

[9] L.-Z. Zhang and Z.-Y. Chen, "Convective heat transfer in cross-corrugated triangular ducts under uniform heat flux boundary conditions," *International Journal of Heat and Mass Transfer*, vol. 54, no. 1–3, pp. 597–605, 2011.

[10] W. M. Kays and A. L. London, *Compact Heat Exchangers*, McGraw-Hill, New York, NY, USA, 3rd edition, 1984.

[11] C. W. Leung and S. D. Probert, "Forced-convective internal cooling of a horizontal equilateral-triangle cross-sectioned duct," *Applied Energy*, vol. 50, no. 4, pp. 313–321, 1995.

[12] L.-Z. Zhang, "Laminar flow and heat transfer in plate-fin triangular ducts in thermally developing entry region," *International Journal of Heat and Mass Transfer*, vol. 50, no. 7-8, pp. 1637–1640, 2007.

[13] P. Talukdar and M. Shah, "Analysis of laminar mixed convective heat transfer in horizontal triangular ducts," *Numerical Heat Transfer Part A: Applications*, vol. 54, no. 12, pp. 1148–1168, 2008.

[14] A. Lawal, "Mixed convection heat transfer to power law fluids in arbitrary cross-sectional ducts," *Journal of Heat Transfer*, vol. 111, no. 2, pp. 399–406, 1989.

[15] G. E. Schneider and B. L. LeDain, "Fully developed laminar heat transfer in triangular passages," *Journal of energy*, vol. 5, no. 1, pp. 15–21, 1981.

[16] R. W. Hanks and R. C. Cope, "Laminar-Turbulent Transitional Flow Phenomena in Isosceles Triangular Cross-section Ducts," *AIChE Journal*, vol. 16, no. 4, pp. 528–535, 1970.

[17] C. A. C. Altemani and E. M. Sparrow, "Turbulent heat transfer and fluid flow in an unsymmetrically heated triangular duct," *Journal of Heat Transfer*, vol. 102, no. 4, pp. 590–597, 1980.

[18] C. W. Leung, T. T. Wong, and H. J. Kang, "Forced convection of turbulent flow in triangular ducts with different angles and surface roughnesses," *Heat and Mass Transfer*, vol. 34, no. 1, pp. 63–68, 1998.

[19] M. Sharabi, W. Ambrosini, S. He, and J. D. Jackson, "Prediction of turbulent convective heat transfer to a fluid at supercritical pressure in square and triangular channels," *Annals of Nuclear Energy*, vol. 35, no. 6, pp. 993–1005, 2008.

[20] C. L. Chaves, J. N. N. Quaresma, E. N. Macêdo, L. M. Pereira, and J. A. Lima, "Forced convection heat transfer to power-law non-Newtonian fluids inside triangular ducts," *Heat Transfer Engineering*, vol. 25, no. 7, pp. 23–33, 2004.

[21] O. Manca, S. Nardini, D. Ricci, and S. Tamburrino, "Numerical investigation on mixed convection in triangular cross-section ducts with nanofluids," *Advances in Mechanical Engineering*, vol. 2012, Article ID 139370, 13 pages, 2012.

[22] K. Rehme, "Simple method of predicting friction factors of turbulent flow in non-circular channels," *International Journal of Heat and Mass Transfer*, vol. 16, no. 5, pp. 933–950, 1973.

[23] Y. G. Lai, "An unstructured grid method for a pressure-based flow and heat transfer solver," *Numerical Heat Transfer, Part B: Fundamentals*, vol. 32, no. 3, pp. 267–281, 1997.

[24] S. Chen, T. L. Chan, C. W. Leung, and B. Yu, "Numerical prediction of laminar forced convection in triangular ducts with unstructured triangular grid method," *Numerical Heat Transfer Part A: Applications*, vol. 38, no. 2, pp. 209–224, 2000.

[25] R. K. Shah and A. L. London, *Laminar Flow Forced Convection in Ducts*, Academic Press, New York, NY, USA, 1978.

[26] B. D. Aggarwala and M. K. Gangal, "Laminar flow development in triangular ducts," *Transactions of the Canadian Society for Mechanical Engineering*, vol. 3, no. 4, pp. 231–233, 1975.

[27] T. Yilmaz and E. Cihan, "General equation for heat transfer for laminar flow in ducts of arbitrary cross-sections," *International Journal of Heat and Mass Transfer*, vol. 36, no. 13, pp. 3265–3270, 1993.

[28] R. Lakshminarayanan and A. Haji-Sheikh, "Extended graetz problems in irregular ducts," *ASME Heat Transfer Division, HTD*, vol. 96, pp. 475–482, 1988.

[29] P. Wilbulswas, *Laminar-flow heat transfer in non-circular ducts [Ph.D. thesis]*, London University, London, UK, 1966.

[30] M. E. Ali and H. Al-Ansary, "Natural convection heat transfer from vertical triangular ducts," in *Proceedings of the ASME Summer Heat Transfer Conference (HT '09)*, vol. 2, pp. 421–428, July 2009.

Downloaded from ade.sagepub.com at University of Otago Library on July 24, 2015

[31] A. E. Bergles, "Some perspective on enhanced heat transfer, second-generation heat transfer technology," *ASME Journal of Heat Transfer*, vol. 110, pp. 1082–1096, 1998.

[32] S. U. S. Choi, "Enhancing thermal conductivity of fluid with nanoparticles," in *Developments and Applications of Non-Newtonian Flows*, D. A. Siginer and H. P. Wang, Eds., FED,V. 231/MD, 66, pp. 99–105, ASME, New York, NY, USA, 1995.

[33] S. U. S. Choi, "Nanofluids: from vision to reality through research," *Journal of Heat Transfer*, vol. 131, no. 3, Article ID 033106, pp. 1–9, 2009.

[34] R. Taylor, S. Coulombe, T. Otanicar et al., "Small particles, big impacts: a review of the diverse applications of nanofluids," *Journal of Applied Physics*, vol. 113, no. 1, Article ID 011301, 2013.

[35] A. Celen, A. Çebi, M. Aktas, O. Mahian, A. S. Dalkilic, and S. Wongwises, "A review of nanorefrigerants: flow characteristics and applications," *International Journal of Refrigeration*, vol. 44, pp. 125–140, 2014.

[36] I. M. Shahrul, I. M. Mahbubul, S. S. Khaleduzzaman, R. Saidur, and M. F. M. Sabri, "A comparative review on the specific heat of nanofluids for energy perspective," *Renewable and Sustainable Energy Reviews*, vol. 38, pp. 88–98, 2014.

[37] O. A. Alawi, N. A. C. Sidik, H. A. Mohammed, and S. Syahrullail, "Fluid flow and heat transfer characteristics of nanofluids in heat pipes: a review," *International Communications in Heat and Mass Transfer*, vol. 56, pp. 50–62, 2014.

[38] A. M. Hussein, K. V. Sharma, R. A. Bakar, and K. Kadirgama, "A review of forced convection heat transfer enhancement and hydrodynamic characteristics of a nanofluid," *Renewable and Sustainable Energy Reviews*, vol. 29, pp. 734–743, 2014.

[39] Y. Xuan and Q. Li, "Heat transfer enhancement of nanofluids," *International Journal of Heat and Fluid Flow*, vol. 21, no. 1, pp. 58–64, 2000.

[40] O. Manca, S. Nardini, and D. Ricci, "A numerical study of nanofluid forced convection in ribbed channels," *Applied Thermal Engineering*, vol. 37, pp. 280–292, 2012.

[41] P. Keblinski, R. Prasher, and J. Eapen, "Thermal conductance of nanofluids: is the controversy over?" *Journal of Nanoparticle Research*, vol. 10, no. 7, pp. 1089–1097, 2008.

[42] J. Buongiorno, D. C. Venerus, N. Prabhat et al., "A benchmark study on the thermal conductivity of nanofluids," *Journal of Applied Physics*, vol. 106, Article ID 094312, 2009.

[43] W. Yu, D. M. France, E. V. Timofeeva, D. Singh, and J. L. Routbort, "Thermophysical property-related comparison criteria for nanofluid heat transfer enhancement in turbulent flow," *Applied Physics Letters*, vol. 96, no. 21, Article ID 213109, 2010.

[44] N. Prabhat, J. Buongiorno, and L.-W. Hu, "Convective heat transfer enhancement in nanofluids: real anomaly or analysis artifact?" in *Proceedings of the ASME/JSME 8th Thermal Engineering Joint Conference (AJTEC '11)*, Honolulu, Hawaii, USA, March 2011.

[45] S. Z. Heris, S. H. Noie, E. Talaii, and J. Sargolzaei, "Numerical investigation of Al_2O_3/water nanofluid laminar convective heat transfer through triangular ducts," *Nanoscale Research Letters*, vol. 6, article 179, 2011.

[46] H. A. Mohammed, N. I. Om, N. H. Shuaib, A. K. Hussein, and R. Saidur, "The application of nanofluids on three dimensional mixed convection heat transfer in equilateral triangular duct," *International Journal of Heat and Technology*, vol. 29, no. 2, pp. 3–12, 2011.

[47] Z. Edalati, S. Zeinali Heris, and S. H. Noie, "The study of laminar convective heat transfer of CuO/water nanofluid through an equilateral triangular duct at constant wall heat flux," *Heat Transfer—Asian Research*, vol. 41, no. 5, pp. 418–429, 2012.

[48] S. Z. Heris, F. Ahmadi, and O. Mahian, "Pressure drop and performance characteristics of water-based Al_2O_3 and CuO nanofluids in a triangular duct," *Journal of Dispersion Science and Technology*, vol. 34, no. 10, pp. 1368–1375, 2013.

[49] S. Z. Heris, Z. Edalati, S. H. Noie, and O. Mahian, "Experimental investigation of Al_2O_3/water nanofluid through equilateral triangular duct with constant wall heat flux in laminar flow," *Heat Transfer Engineering*, vol. 35, no. 13, pp. 1173–1182, 2014.

[50] S. K. Das, S. U. S. Choi, W. Yu, and T. Pradeep, *Nanofluids Science and Technology*, John Wiley & Sons, Hoboken, NJ, USA, 2008.

[51] W. M. Rohsenow, J. P. Hartnett, and Y. I. Cho, *Handbook of Heat Transfer*, McGraw-Hill, New York, NY, USA, 3rd edition, 1998.

[52] K. Khanafer and K. Vafai, "A critical synthesis of thermophysical characteristics of nanofluids," *International Journal of Heat and Mass Transfer*, vol. 54, no. 19-20, pp. 4410–4428, 2011.

[53] B. C. Pak and Y. I. Cho, "Hydrodynamic and heat transfer study of dispersed fluids with submicron metallic oxide particles," *Experimental Heat Transfer*, vol. 11, no. 2, pp. 151–170, 1998.

[54] S.-Q. Zhou and R. Ni, "Measurement of the specific heat capacity of water-based Al_2O_3 nanofluid," *Applied Physics Letters*, vol. 92, no. 9, Article ID 093123, 2008.

[55] K. Khanafer, K. Vafai, and M. Lightstone, "Buoyancy-driven heat transfer enhancement in a two-dimensional enclosure utilizing nanofluids," *International Journal of Heat and Mass Transfer*, vol. 46, no. 19, pp. 3639–3653, 2003.

[56] M. Corcione, "Empirical correlating equations for predicting the effective thermal conductivity and dynamic viscosity of nanofluids," *Energy Conversion and Management*, vol. 52, no. 1, pp. 789–793, 2011.

[57] Fluent, *FLUENT Computational Fluid Dynamic Code Version 6.3 User Guide*, 2006, http://www.fluent.com/.

[58] D. P. Fleming and E. M. Sparrow, "Flow in the hydrodynamic entrance region of ducts of arbitrary cross section," *Journal of Heat Transfer*, vol. 91, pp. 345–354, 1969.

[59] R. W. Miller and L. S. Han, "Pressure losses for laminar flow in the entrance region of ducts of rectangular and equilateral triangular cross section," *Journal of Applied Mechanics*, vol. 38, no. 4, pp. 1083–1087, 1971.

[60] S. Ferrouillat, A. Bontemps, J.-P. Ribeiro, J.-A. Gruss, and O. Soriano, "Hydraulic and heat transfer study of SiO_2/water nanofluids in horizontal tubes with imposed wall temperature boundary conditions," *International Journal of Heat and Fluid Flow*, vol. 32, no. 2, pp. 424–439, 2011.

Downloaded from ade.sagepub.com at University of Otago Library on July 24, 2015